

Article

Rapid Recruitment of Symbiotic Algae into Developing Scleractinian Coral Tissues

Thomas Bockel^{1,2} and Baruch Rinkevich^{1,*} ¹ National Institute of Oceanography, Tel Shikmona, PO Box 8030, Haifa 31080, Israel² Laboratory for Biological Geochemistry, School of Architecture, Civil and Environmental Engineering, Ecole Polytechnique Fédérale de Lausanne, CH-1015 Lausanne, Switzerland

* Correspondence: buki@ocean.org.il; Tel.: +972-4-856-5275

Received: 31 July 2019; Accepted: 3 September 2019; Published: 4 September 2019



Abstract: While the early acquisition of Symbiodiniaceae algae into coral host tissues has been extensively studied, the dynamics of the migration of algal cells into rapidly expanding coral tissues still lacks a systematic study. This work examined two Red Sea branching coral species, *Pocillopora damicornis* and *Stylophora pistillata*, as they were growing and expanding their tissue laterally on glass slides (January–June, 2014; 450 assays; five colonies/species). We measured lateral tissue expansion rates and intratissue dinoflagellate migration rates. Tissue growth rates significantly differed between the two species (with *Stylophora* faster than *Pocillopora*), but not between genotypes within a species. Using a “flow-through coral chamber” under the microscope, the migration of dinoflagellates towards the peripheral edges of the expanding coral tissue was quantified. On a five-day timescale, the density of the endosymbiotic dinoflagellate cells, presenting within a 90 µm region of expanding coral tissue (outer edge), increased by a factor of 23.6 for *Pocillopora* (from 1.2×10^4 cells cm^{-2} to 2.4×10^5 cells cm^{-2}) and by a factor of 6.8 for *Stylophora* (from 3.6×10^4 cells cm^{-2} to 2.4×10^5 cells cm^{-2}). The infection rates were fast (5.2×10^4 and 4.1×10^4 algal cells $\text{day}^{-1} \text{cm}^{-2}$, respectively), further providing evidence of an as yet unknown pathway of algal movement within coral host tissues.

Keywords: algal movement; coral tissue; endosymbiont proliferation; lateral skeleton preparative; nubbin assay; *Pocillopora*; Red Sea; *Stylophora*; Symbiodiniaceae

1. Introduction

Hermatypic (reef-building) corals have developed mutualistic relationships with unicellular, photosynthesizing, endosymbiotic dinoflagellate algae of the family Symbiodiniaceae [1] (often referred to as zooxanthellae). Symbionts are acquired primarily into the oral gastrodermal cells during early ontogeny, via horizontal (from the surrounding seawater; usually in broadcasting species) or vertical transmission (maternal inheritance; usually in brooding species) [2,3]. The endosymbiotic dinoflagellates found in corals are typically 8–12 µm diameter cells that reside exclusively in membrane-bound vacuoles in the gastrodermal cells as nonmotile cells, lacking flagella [4]. The density of these endosymbiotic dinoflagellates typically reaches $1\text{--}2.5 \times 10^6$ cells cm^{-2} in adult hermatypic corals [5], although this is probably highly variable on both temporal and spatial scales [4,6]. These cells provide the coral host with a large portion of its daily energy needs [7]. This symbiosis is thus of fundamental importance to the ecological fitness of coral reefs, and it is clear from a multitude of studies that the coral-algal relationship is highly dynamic and flexible, primarily with respect to recruitment/infection, expulsion, cell division, and interhost (re-)distribution of the algae [8].

Despite its ecological importance, very little is known about the origin of algal infections into newly developed tissues (that is, either from the environment or via algal-infected tissue), or the

mechanisms that govern algal invasion into coral tissues [8]. In a study on the sea anemone *Exaiptasia pallida* [9], lacerates of algal-infected anemones developed within a short period of a few days into juvenile anemones, where algal cells were re-distributed to the developing tentacles (the sites they can predominantly be found in adult anemones). The above literature and the prevailing scheme describe infections by Symbiodiniaceae algae through the mouths of the host polyps, where contacts with the coral tissues continues with phagocytoses of algal cells into the gastrodermal cells [8,10,11]. However, studies of symbiont acquisition into newly developed coral tissues are challenging, fraught with various technical limitations, which stem from the nontransparent nature of the tissue covering the calcareous skeleton [12], the intrinsic difficulties in working with corals even under controlled laboratory conditions, and the near-infeasibility of maintaining healthy full aposymbiotic adult colonies on a long-term basis in preparation for subsequent re-infection assays [13].

The present study offers quantitative data on the migration of symbiotic microalgae into naturally expanding coral tissues. Previous studies have shown that algal recruitment and repopulation of bleached corals under natural conditions are processes that have a duration measured in weeks [8,14]. In contrast, other studies on soft corals [10,15,16] have documented fast movement of endosymbionts through the tissues, coenenchyme, and gastrovascular system of soft corals, with the latter functioning as an effective, albeit primitive, vascular system (also found in hard corals) [17]. Fast intracolony symbiont migration has also been observed in *Acropora cervicornis* [18] and in *Montipora capitata* [19], as well as in ultraviolet-A irradiated and thermally challenged *Pocillopora* sp. tissues [20]; in the latter study the dinoflagellates first migrated into the coral coenenchyme, before making their way into the gastrovascular cavity.

Literature suggests that following a bleaching event, bleached coral tissues may be repopulated by Symbiodinium algae via oral invasions (by free-living zooxanthellae) and/or via the cell divisions of residual remaining algal cells in coral tissues. Muller-Parker et al. (2015) further posited that the growth of zooxanthellae in coral tissues must somehow be regulated relative to the growth of the host. Several studies have indeed documented the colonization patterns of algal cells into algal-poor tissues, such as the new polyps/tissues of growing branching coral colonies [21–23]. Regrettably, despite the overwhelming number of studies on coral/algal symbiosis, our knowledge of how the symbiotic algae colonize new tissues is far from complete.

Here, we propose the rapid migration of symbiotic algae as a major way of colonizing newly developing coral tissues. To document and to elucidate routes of algal infections into newly formed coral tissues, we used the Lateral Skeleton Preparative (LSP) assay [12,24,25] (Figure 1a,b), in which observations were made on newly formed flat and transparent coral tissues spread on glass slides. This allowed us to closely track the sequence of events that are associated with algal acquisition. Using this LSP assay on nubbins from two Red Sea branching coral species, *Pocillopora damicornis* and *Stylophora pistillata*, we studied zooxanthellae recruitment rates into substratum-spreading new tissues at the levels of colony and species. We analyzed the gradients of symbiotic cell abundance along axes from peripheral sites towards the centers of the spreading tissues, as well as the zooxanthella vertical distributions at marginal coral tissues.

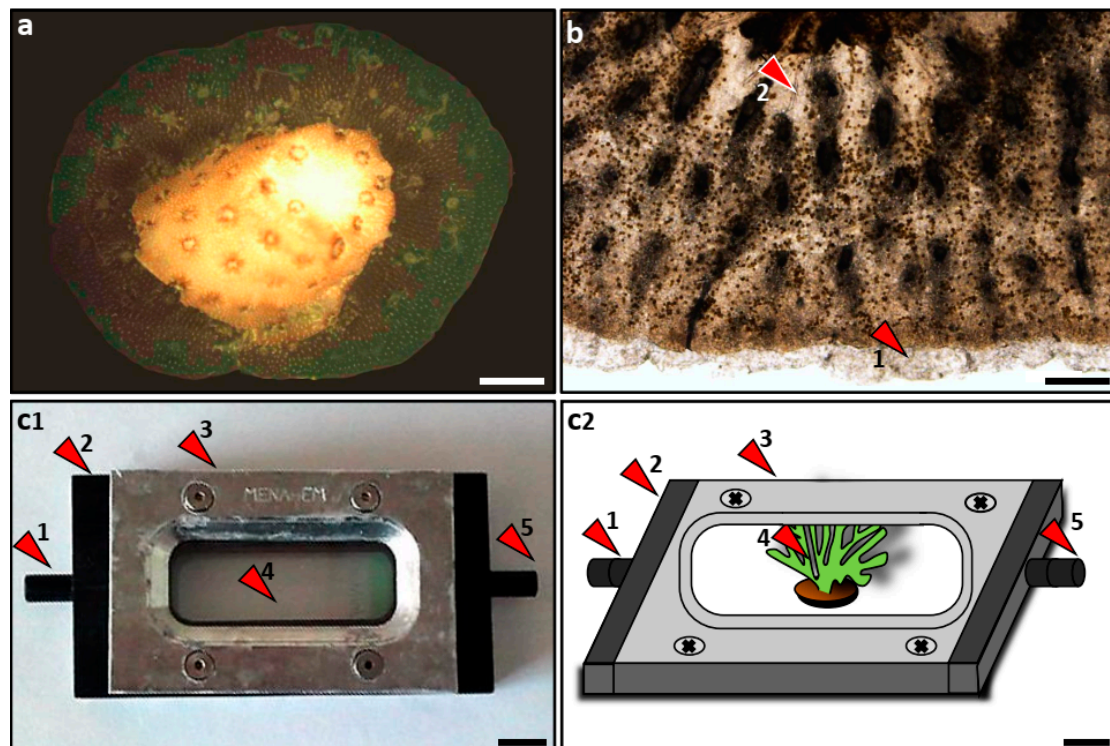


Figure 1. (a). An established nubbin (lateral skeleton preparative; LSP) assay, with the lateral extension on the substratum (a glass slide). (b) RGB image of the edge of the spreading tissue ($\times 40$), with newly formed noncalcified tissue (1) and zooxanthellae (2); age of the nubbin: 60 days. (c1), (c2): A photograph (c1) and illustration (c2) of the flow-through “coral chamber”, with the inlet (arrowhead 1), the central plastic box (arrowhead 2), the top sealing metal plate (arrowhead 3), the top cover glass slide (arrowhead 4) with the LSP below and the outlet (arrowhead 5). Scale bars: a = 2 mm; b = 0.2 mm; c1, c2 = 1 cm.

2. Materials and Methods

We used colonies of two common Indo Pacific pocilloporid species, *Pocillopora damicornis* and *Stylophora pistillata*. Five colonies of each species (most probably genotypes; each colony represented only a single genet, since detached and scattered colonial fragments of pocilloporid species in Eilat do not survive) [26] were collected from the coral nursery, suspended mid-water at a depth of 10 m [27] in the north beach of Eilat, Red Sea, under a permit from the Israeli Nature Reserve Authority (permit no 2014/29995). The colonies were transported to the laboratory at the Israel Oceanographic and Limnological Research institute (IOLR, Haifa) in insulated containers and kept in a controlled temperature (25 °C) running seawater system until used (January–June, 2014). The lighting conditions were controlled by Metal Halide cool white (150 W, Philips IP65) in a 12:12 h light:dark regimen, administered by the use of three types of fluorescent tubes (Cool White, Fluora and Blue-Blue, Osram, Germany).

2.1. Nubbin Preparation

For the research, we used nubbin-size fragments, a protocol that reduces to minimum the impacts on donor colonies [28]. All the experiments were performed at the laboratory at IOLR. Coral nubbins were prepared according to the nubbin assay [28] (Figure 1a), where coral branches were cut into small pieces, approximately 0.25 cm² each, using a wire cutter. The exposed skeleton side of each nubbin cut was dried with a paper towel for a few seconds. Glass slides labeled with the genotypes' number (no 1–5 species⁻¹) were scratched with a diamond pen to improve nubbin attachment, and three nubbins were glued on each slide ca. 1 cm apart) using Loctite Superglue.

Three sets of nubbin slides were generated, with a two-week interval between them (set one at day 0, set two at day 15 and set three at day 30). Each set consisted of 15 nubbins per coral genotype, totaling 75 nubbins per experimental set-up for each of the two species. The maintenance of the nubbins during the experimental period (60 d) consisted of a thorough weekly cleaning of the slides, using razor blades and thin painting brushes to remove the turf algae. The nubbins were fed twice a week using *Artemia salina* nauplii.

2.2. Lateral Tissue Extensions

The glued nubbins formed lateral tissue extensions within three weeks, that firmly attached them to the substratum [12,28] (Figure 1a,b). The lateral tissue extensions (added surface areas) were monitored in order to establish average growth rates per species and genotype (using a Nikon SMZ 1000 stereomicroscope equipped with DeltaPix Invenio 3s II camera at a magnification of $\times 8$) on 20% of the nubbins for each set of experiments after 30, 45, and 60 days. We also photographed and measured the surface areas of all the nubbins at day 45 (the laterally extended tissues on the glass slides) in each experimental set. These photographs were digitized and analyzed using the Coral Point Count software (CPCe), developed by the American National Coral Reef Institute [29]. The impacts of species and genotype on growth rates were calculated for each nubbin from all the experimental sets at day 45. The metadata of the spreading tissue surface areas and the survival per species/genotype were determined for each set of photographs. Statistical analyses were performed using the R statistical software (R Core Team 2016; <https://www.R-project.org>).

2.3. Live Tissue Observations

Observations under the microscope of in vivo live tissue on horizontally spreading coral tissues (lasting about 10 min each) were made by using a flow-through “coral chamber” (Figure 1c,d), consisting of a rigid plastic box opened on the top and bottom. When in use, the chamber was closed on the bottom side by a glass slide carrying nubbins, and by a microscope cover glass on top. Both sides were sealed with metal plates and sealing rubbers, while the inlet of the chamber was connected by a 0.5 m plastic tube to a ViaAqua VA80 water pump, placed in a plastic tank filled with running, temperature-controlled filtered seawater, maintained at 25 °C with a Hydrosafe plus water heater. The chamber’s outlet was connected to the tank with a 1 m plastic tube. The water flow through the coral chamber was maintained at the maximum level, allowing the polyps to open. The state of coral/algal tissues during the experiment was photographed using a DeltaPix Invenio 3s II camera, attached to a Nikon eclipse e200 microscope at a magnification of $\times 40$.

2.4. Zooxanthella Observations

Stylophora pistillata colonies from the shallow waters in the Gulf of Eilat associate with Symbiodiniaceae [1] from the genera *Symbiodinium* (formerly clade A) [3]. In order to study the algal cell densities/distributions in the spreading coral tissues, photographs were taken with an Olympus DP 73 camera, attached to an Olympus Bx 50 microscope (40 \times magnification). Images of spreading tissue edges were captured without a filter under normal light, and fluorescence imaging was conducted under fluorescent light (Olympus U-RFL-T) using a green fluorescence Olympus UMNG filter, combining a 530 to 550 nm band pass excitation filter for the green excitation of the coral tissue pigments, and a 590 nm barrier filter for the red fluorescence emission of the chlorophyll (OLYMPUS; www.olympus-global.com). The fluorescent images were then analyzed using the Matlab software and a custom-made algorithm, allowing the zooxanthellae’s automatic counting to create raster maps that showed algal locations. This was performed by transforming the images from the standard Red Green Blue colors to grayscale images that were processed into binary images, and calculating their Euclidean distances to the nearest nonzero pixel, counting algae using the “watershed” function (Figure S1a–f).

2.5. Endosymbiotic Dinoflagellate Recruitment

Endosymbiotic dinoflagellates recruitment to the newly developing coral tissues was determined by measuring endosymbionts cell numbers (per unit area) at the edge of the spreading tissues, using snapshots taken at days 0 and 5. Observations were performed on four nubbins from each genotype for each species (nested analysis using F-ratios), along experimental sets one and two. Photographs of spreading peripheral tissue edges (Figure 1b) were taken using an Olympus DP 73 camera, attached to an Olympus Bx 50 microscope at a magnification of $\times 40$, using standard illumination and a fluorescence Olympus lamp (U-RFL-T) with a green fluorescence filter (Olympus, UMNG; 2 pictures/specimen/d over a period of 5 days). The images were processed for density measurements using the Matlab software, and each image was separated into frames of 40 by 40 pixels, resulting in a frame size of approximately $45 \mu\text{m}$. The frames were processed, using the same zooxanthellae localization algorithm, in order to reveal the number of symbiotic cells per frame. A gradient in the number of endosymbionts per unit area/nubbin was developed along a trajectory line of frames, from the marginal zones towards the nubbin's center.

2.6. Algal Cell Counting

Three nubbins with different genotypes from each species were carefully detached from the glass slides using a razor blade, and the remaining spreading tissues were photographed under the stereomicroscope (magnification $\times 8$) with a DeltaPix Invenio 3s II camera. These images were used to discern the surface area of the spreading tissue by using the CPCe software. To separate the tissue from the skeleton, each of the paired nubbins and their corresponding spreading tissue were then placed separately for approximately 10 min into calcium/magnesium-free seawater containing an ethylene diamine tetra acetic acid (EDTA) solution (Na_2HSO_4 7 mmol L^{-1} , NaHCO_3 0.2 mmol L^{-1} , Tris HCl 20 mmol L^{-1} , KCl 10 mmol L^{-1} , NaCl 540 mmol L^{-1} and EDTA 20 mmol L^{-1} (pH 8.2)). Tissue detachment was further assisted by rinsing the specimen with repeated jets of filtered seawater from a pipette. This procedure did not alter cell integrity [30]. The solution that contained the individual dispersed cells was transferred to a test tube, diluted with filtered seawater, and centrifuged under 20°C for 10 min at 2000 rpm. The supernatant was then removed, leaving the cell pellet, which was stained for DNA with Hoechst at a concentration of $1 \mu\text{l ml}^{-1}$. The volume of the obtained solution was measured, and the solution was kept in the dark. Cell counts (symbiotic and host cells) were produced shortly after the preparation of the samples using a Neubauer hemocytometer (repeated 5 times/sample).

The surface areas of the spreading tissues were measured using the CPCe software, and the measurements of the nubbin surface areas were performed according to the aluminum foil wrapping method [31]. The weights of the aluminum foil were compared with a calibrated curve, created by weighing five aluminum foil squares with respective areas of 0.5, 1, 2, 2.5, and 5 cm^2 . Results were calculated as cell numbers/square surface area.

2.7. Histology

Histological sections were performed following decalcification on the two-dimensional (2D) flat growing tissues of *Pocillopora damicornis* and *Stylophora pistillata* (2 nubbins/species, with different genotypes), concentrating on the area between the polyps' tissues. Nubbins were fixed in Bouin's solution (24 hours), and the partly detached tissues were removed from the skeletons using forceps, rinsed in filtered seawater, and then processed into traditional paraffin-embedded samples, with $5 \mu\text{m}$ thickness serial sections. The sections were attached to Marienfeld microscope slides covered with thin poly L-Lysine and stained with Ehrlich hematoxylin and eosin. The results were viewed with an Olympus Bx50 microscope and photographed with a digital Olympus DP73 camera.

3. Results

3.1. Forming Lateral Tissue Sheets

A considerable number of nubbins (75% for *S. pistillata* and 33% for *P. damicornis*) developed fast-growing lateral and transparent tissue extensions on the glass slides within three to four weeks (initially lacking zooxanthellae and calcium carbonate crystals) that firmly attached them to the substratum (Table 1). As previous studies have documented the formation of almost 100% lateral tissue sheets on substratum [24,25], the somewhat lower success rate here might be a result of excessive application of glue on the substratum during preparation, delaying fast horizontal tissue growth. Nevertheless, survival of nubbins during the 45 days of observation was very high, with mortality of only 11% for the *P. damicornis* nubbins and 0.5% for the *S. pistillata* nubbins (Table 1). The newly formed tissue sheets started to calcify with time, forming thin disks of skeletons and tissues on the substratum, each approximately 2 cm in diameter.

Table 1. The performance of the nubbins (survival, established LPS), sorted according to the different genotypes/coral species, on day 45. LPS-Lateral Skeleton Preparative [12].

Species	Genotype	Nubbins (n)	Mortality		Developing LPS		LPS Lateral Sizes		
			n	% of Initial	n	% of Alive	< 40 mm ²	40–100 mm ²	> 100 mm ²
<i>P. damicornis</i>	1	38	0	0	14	37	10	3	1
	2	42	2	5	10	25	9	1	0
	3	41	5	12	19	53	19	0	0
	4	44	12	27	7	22	7	0	0
	5	44	4	9	12	30	12	0	0
	Total/%	209	23	11	62	33	57	4	1
<i>S. pistillata</i>	1	45	0	0	28	62	24	4	0
	2	44	0	0	33	75	26	6	1
	3	43	1	2	27	64	23	3	1
	4	43	0	0	29	67	24	4	1
	5	45	0	0	27	60	20	6	1
	Total/%	220	1	0.5	144	66	117	23	4

Twenty-seven of the *P. damicornis* nubbins and 30 of the *S. pistillata* nubbins were each monitored throughout a 2 month period (Figure 2a). Two of these *P. damicornis* nubbins died, and 13 did not develop lateral tissue extensions, compared with a 100% survival rate and 11 nubbins that did not form lateral tissue extensions in *S. pistillata*. We followed (Figure 2a) 12 *P. damicornis* and 19 *S. pistillata* nubbins, revealing, after 30, 45, and 60 days, spreading surface areas (means ± SD) of 2.6, 8.2 and 15 mm² (±2.4, 11, and 15 mm², respectively) for *P. damicornis*, and 9.2, 17, and 27 mm² (±7, 15, and 22 mm², respectively) for the *S. pistillata* nubbins. Mean growth rates measured at day 60 were 0.57 ± 0.74 mm² d⁻¹ for *P. damicornis* and 0.85 ± 0.75 mm² d⁻¹ for *S. pistillata*. The growth rates show that *S. pistillata* produced significantly larger lateral tissue extensions ($p < 0.05$, standard parametric nested ANOVA; 45 d from fixation on the substratum). No significant effect of genotype was found ($p > 0.05$; *S. pistillata* and *P. damicornis*).

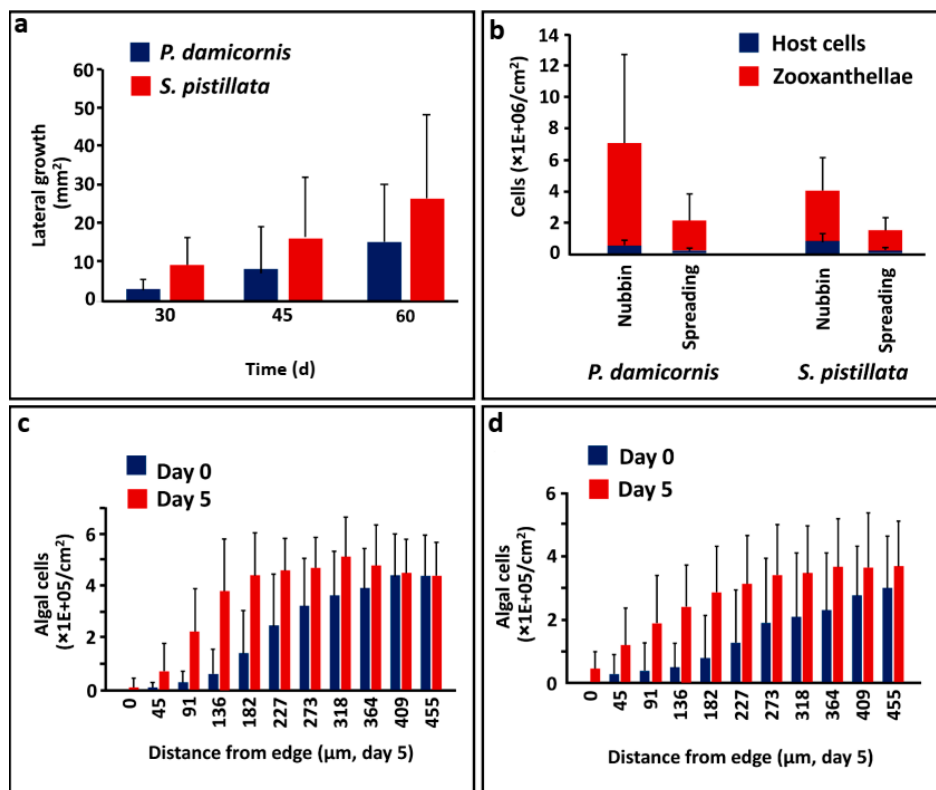


Figure 2. Tissue growth on the substratum (genotypes averaging). (a) The average lateral surface areas of *S. pistillata* (n = 19) and *P. damicornis* (n = 12) nubbins after 30, 45, and 60 days. (b) Endosymbiotic dinoflagellates and host cell numbers cm⁻² in the nubbins and spreading tissues of *P. damicornis* and *S. pistillata*. (c) Variations (5 day intervals) in endosymbiotic dinoflagellate numbers within *P. damicornis*' peripheral spreading tissues, 0–455 µm from the most distal lines. Same tissue sites after 5 days of growth. (d) Variations (5 day intervals) in endosymbiotic dinoflagellate numbers within *S. pistillata*'s peripheral spreading tissues, 0–455 µm from the most distal lines. Same tissue sites after 5 days of growth. (Error bars = SD).

Observations of lateral growth of nubbins taken from the two coral species using the flow-through coral chamber showed that the distal and newly formed thin and transparent tissue extensions on the substratum (Figure 1b) were devoid of endosymbiotic dinoflagellates. These lateral extensions were decidedly active, performing frequent expansion–retraction motions of the tissue gliding on the substratum surface, with an amplitude of a few micrometers (Figure S2a,b,c). In addition, these observations showed that endosymbiotic dinoflagellate cells were rapidly transported into the algal-free coral tissues on the substratum within a few minutes of the onset of observations, relocated from established tissues in the nubbins. The presence of new endosymbiotic dinoflagellates in the edge areas of tissues, previously devoid of symbiotic cells, was observed within a few minutes of onset of observations (Supp. Figure S2d,e,f).

The study of recruitment of endosymbiotic dinoflagellates into newly formed coral tissues was performed by counting the number of symbiotic algal cells in a 5 d interval protocol, within the most distal 500 μm expanded edges of the lateral spreading tissues. In the 90 μm outermost peripheral zones of the studied nubbins, algal numbers increased by ca. 24 and 7 times for *P. damicornis* and *S. pistillata*, respectively (Figure 2c,d). A clear gradient in the numbers of endosymbiotic dinoflagellates was observed in the 500 μm outermost peripheral spreading tissue in both species, levelling for *P. damicornis* at about 4.5×10^5 cells cm^{-2} in the ca. 250 μm from the tissue edge zone (Figure 2c), and for *S. pistillata*, about 3.5×10^5 cells cm^{-2} at the levelling distance of about 400 μm from the edge (Figure 2d). The infection rate of algal cells at the edge of the tissue was 5.2×10^4 algal cells $\text{d}^{-1}\text{cm}^{-2}$ for *P. damicornis* and 4.1×10^4 algal cells $\text{d}^{-1}\text{cm}^{-2}$ for *S. pistillata*.

3.2. Algal Cells in Coral Tissues

Endosymbiotic dinoflagellates and host cell counts in the LPS of both coral species were measured on day 45 (Figure 2b), revealing for *P. damicornis* 4.0×10^5 algal cells cm^{-2} ($\pm 4.2 \times 10^5$) within the nubbins and 1.3×10^5 cells cm^{-2} algal cells ($\pm 1.0 \times 10^5$) in the spreading tissues, compared with 6.9×10^6 host cells cm^{-2} ($\pm 5.9 \times 10^6$) within the nubbins and 2.1×10^6 host cells cm^{-2} ($\pm 1.8 \times 10^6$) in the spreading tissues. For *S. pistillata* we counted 8.6×10^5 algal cells cm^{-2} ($\pm 4.7 \times 10^5$) in the nubbins and 2.2×10^5 algal cells cm^{-2} ($\pm 1.6 \times 10^5$) in the spreading tissues, compared with 3.4×10^6 host cells cm^{-2} ($\pm 2.2 \times 10^6$) in the nubbins ($\pm 2.2 \times 10^6$) and 1.4×10^6 host cells cm^{-2} ($\pm 8.4 \times 10^5$) in the spreading tissues. Endosymbiotic dinoflagellates versus animal cell ratios for *P. damicornis* were 0.058 in the nubbins and 0.062 in the spreading tissues, and for *S. pistillata* they were 0.25 in the nubbins and 0.14 in the spreading tissues, revealing nonmatching trajectories for endosymbionts recruitment into the newly established tissues of different coral species.

3.3. Algal Cells in Histological Sections

Endosymbiotic dinoflagellate distribution in the two gastroderm layers (the oral and the aboral gastrodermis; Figure 3a) of the newly formed coral tissues was investigated in both studied species on longitudinal sections. Sections were made in parallel to the spreading tissues' peripheral plane (3 mm in diameter) and from three regions across the spreading tissues, starting from the most peripheral radii (0–0.5, 0.5–1.0, 1.0–1.5 mm; Figure 3b). Nine histological sections were analyzed from each region. We recorded length, the number of endosymbiotic dinoflagellates present in the lower gastroderm, and the endosymbiotic dinoflagellates numbers in the oral (upper) gastroderm for each section, resulting in average numbers of symbiotic cells for each layer and region. Zooxanthellae density was calculated using permutational ANOVA, showing significant effect of layer and region (p value < 0.05). No significant effect of "host species" was found. Post-hoc Bonferroni-adjusted tests were performed on layer and region factors. Significantly more endosymbiotic dinoflagellates were recorded in the upper gastroderm compared with the lower gastrodermal layer, which faces the calicoblastic layer in both species (averaging $29,057 \pm 19,196$ algal cells/ cm^{-2} and $26,490 \pm 25,255$ algal cells cm^{-2} in the lower gastroderm versus $167,689 \pm 149,127$ algal cells cm^{-2} and $119,477 \pm 115,327$ cells cm^{-2} in the upper gastroderm, for *P. damicornis* and *S. pistillata*, respectively). This was recorded in all strips, except for the most distal zone (0 to 0.5 mm from the tissue edge), where the difference between the number of endosymbiotic dinoflagellates in the upper and lower gastrodermal layers was not significant ($p > 0.05$).

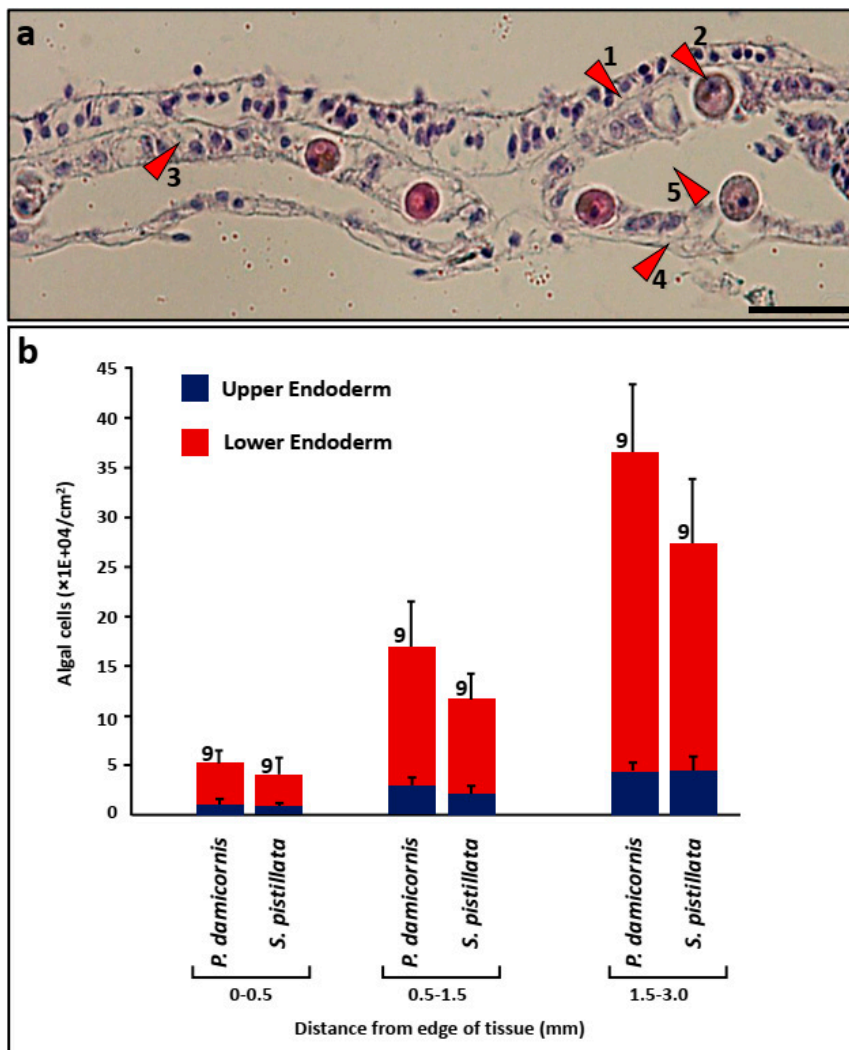


Figure 3. (a). A representative histological section of coral tissue spreading on the substratum, with the epidermis (1), endosymbiotic dinoflagellates (2), upper gastroderm (3), the lower gastroderm (4), and part of the ramifying gastrovascular cavity (canal; 5). Scale bar = 20 μm . (b) Zooxanthella numbers at the 1.5 mm fringed peripheral zone in *P. damicornis* and *S. pistillata* spreading tissues, divided into three marginal belts from the most peripheral extension line towards the center (0–0.5, 0.5–1.0, 1.0–1.5 mm). Numbers along the error bars = number of histological sections analyzed within each marginal belt. PO = *P. damicornis*; ST = *S. pistillata*. Error bars = SD.

4. Discussion

During a bleaching event, corals are very quickly deprived of symbiotic algae [4,8,20], while the recovery of bleached tissues by way of free-living or residual endosymbiotic dinoflagellates (zooxanthellae live within the coral tissues in extremely high densities, greater than $10^6/\text{cm}^2$) is a slow process that can last several months [32], due to the limited number of free-living endosymbiotic dinoflagellates [4,33]. The literature further indicates the relatively slow rates of cell proliferation characteristic to the zooxanthellae [8,34]. The mitotic index of the zooxanthellae inside cnidarian hosts is generally lower than 5% [8], with a reported value of 0.61% for *Stylophora pistillata* [35].

The results of the present study point out that the mode of algal establishment into new coral tissues of the two branching species studied (*P. damicornis* and *S. pistillata*) defies the prevailing tenet. Using the LPS assay approach on *P. damicornis* and *S. pistillata* nubbins, we have demonstrated fast endosymbiotic dinoflagellates recruitment rates (or introduction) into newly formed coral tissues. During the first 5 days, mean (\pm SD) of $93.3 \pm 75.0 \mu\text{m}^{-1}$ of tissue (for *P. damicornis*) and $157.7 \pm 86.7 \mu\text{m}^{-1}$

of tissue (for *S. pistillata*) were added, containing about $42,455 \pm 63,985$ algal cells/cm⁻² (*P. damicornis*) and $76,352 \pm 68,252$ algal cells/cm⁻² (*S. pistillata*) in the most distal 90µm expanded edges of the lateral spreading tissues. Moreover, over a 5 day interval, endosymbiotic dinoflagellate cells in the most distal 90µm expanded tissue edges at day 0 were multiplied 23.6-fold (from $11,488 \pm 27,547$ algal cells cm⁻² to $270,656 \pm 236,342$ algal cells cm⁻²; *P. damicornis*) and 6.8-fold (from $35,553 \pm 59,654$ algal cells cm⁻² to $241,603 \pm 124,130$ algal cells cm⁻²; *S. pistillata*). When considering a standard 3 cm in diameter nubbin, these results imply a recruitment of as many as 8878 algal cells and 7058 algal cells only in the 90µm expanded edges of the lateral spreading tissues (*P. damicornis* and *S. pistillata*, respectively). In fact, endosymbiotic dinoflagellates recruitment in newly formed tissues occurs prior to the formation of the new polyps' mouth (data not shown). These findings and the observable fast movements of algal cells within the coral tissues attest to the translocation of algal phalanges during the development of spreading tissues in their hundreds of thousands, and even millions in total. These algal cells are primarily transferred from internal reservoirs and/or from the freely circulating masses in established tissues [10,14–16,36] and to a lesser extent from environmentally acquired zooxanthellae, due to the low density of endosymbiotic dinoflagellates present in the water column [33]. Considering that algal density in the developing coral tissues increases rapidly, and that symbiotic algae exhibit a low mitotic rate [8,34], it is further possible that symbiotic cell divisions in expanding tissues exhibit no diurnal pattern like the one often observed in algal assemblages during lateral tissue expansion.

Very little is currently known about how cells are actually transported and how symbiont populations are regulated and controlled in newly formed tissues. Studies on soft corals [10,15,16] revealed that the gastrovascular systems of these corals function as effective circulatory apparatus, analogous to a primitive vascular system, and that free endosymbiotic dinoflagellates and holobionts (a coral cell with one or two symbionts) are circulating throughout different parts of the colonial entity. Further, cells lining the gastrodermis are ciliated, and the “expansion–retraction motion” of tissues we observed may likely serve as the mechanism of transport. Comparable ramifying gastrovascular systems are well characterized in branching corals, primarily in acroporid and pocilloporid corals [17,36]. Yet the exact infection processes of recruiting endosymbiotic dinoflagellates to the right sites still remains elusive. Another possibility, albeit slower, is that some host cells containing symbionts are transported by tissue/morphogenetic movements, similar to the migration of cnidoblasts into hydrozoans' tentacles [37]. Clearly, if corals can rapidly regulate their symbiont pool size in newly growing sites, it can be deduced that they should maintain reserve algal symbionts ready to be translocated into areas poor in endosymbiotic cells, maximizing the net benefit of this symbiosis.

It is commonly perceived that the algal–animal symbiosis in corals is homeostatic in nature, as the number of algal cells in coral tissues remains relatively constant under a given set of environmental conditions, while symbiont abundance is variable in space and time [4,6]. Fast-growing tissues (like branch tips in *Acropora*) [37], encrusting edges of semimassive corals [38] and the lateral growth of attaching coral fragments), must establish this homeostasis as soon as possible, elevating symbiont abundance to the species-specific natural spatiotemporal variability [6,39]. In following the nature of this surprisingly fast algal recruitment into newly formed coral tissues, we postulate the existence of novel control mechanisms that regulate this phenomenon, maximizing biological properties as well as responding to cost/benefit attributes.

Supplementary Materials: The following are available online at <http://www.mdpi.com/2077-1312/7/9/306/s1>, Figure S1: Steps for the endosymbiotic dinoflagellates automatic counting methodology, Figure S2: Tissue and algal movements.

Author Contributions: T.B. performed the research and analyzed the data. B.R. supervised, designed the research, and provided supplies. Both authors wrote and contributed to the paper.

Funding: This research received no external funding.

Acknowledgments: Thanks are due to G. Paz for illustrating the figures and for G. Davidovich, who constructed the first prototype of the “flow-through coral chamber”.

Conflicts of Interest: The authors declare no conflict of interest.

References

1. Lajeunesse, T.C.; Parkinson, J.E.; Gabrielson, P.W.; Jeong, H.J.; Reimer, J.D.; Voolstra, C.R.; Santos, S.R. Systematic Revision of *Symbiodiniaceae* Highlights the Antiquity and Diversity of Coral *Endosymbionts*. *Curr. Boil.* **2018**, *28*, 2570–2580. [[CrossRef](#)]
2. Fitt, W.K. The role of chemosensory behavior of *Symbiodinium microadriaticum*, intermediate hosts, and host behavior in the infection of coelenterates and molluscs with zooxanthellae. *Mar. Boil.* **1984**, *81*, 9–17. [[CrossRef](#)]
3. Karako-Lampert, S.; Katcoff, D.; Achituv, Y.; Dubinsky, Z.; Stambler, N. Do clades of symbiotic *dinoflagellates* in scleractinian corals of the Gulf of Eilat (Red Sea) differ from those of other coral reefs? *J. Exp. Mar. Boil. Ecol.* **2004**, *311*, 301–314. [[CrossRef](#)]
4. Muller-Parker, G.; D'Elia, C.F.; Cook, C.B. Interactions between Corals and Their Symbiotic Algae. In *Coral Reefs in the Anthropocene*; Springer Science and Business Media LLC: Berlin, Germany, 2015; pp. 99–116.
5. Jones, R.J.; Yellowlees, D. Regulation and control of intracellular algae (=zooxanthellae) in hard corals. *Philos. Trans. R. Soc. B Boil. Sci.* **1997**, *352*, 457–468. [[CrossRef](#)]
6. Rowan, R. Review—Diversity and ecology of zooxanthellae on coral reefs. *J. Phycol.* **1998**, *34*, 407–417. [[CrossRef](#)]
7. Muscatine, L. The role of symbiotic algae in carbon and energy flux in reef corals. In *Ecosystems of the World; Coral Reefs*, Dubinsky, Z., Eds.; Elsevier: Amsterdam, The Netherlands, 1990; Volume 25, pp. 75–87.
8. Davy, S.K.; Allemand, D.; Weis, V.M. Cell Biology of Cnidarian-Dinoflagellate Symbiosis. *Microbiol. Mol. Boil. Rev.* **2012**, *76*, 229–261. [[CrossRef](#)]
9. Chen, W.-N.U.; Hsiao, Y.-J.; Mayfield, A.B.; Young, R.; Hsu, L.-L.; Peng, S.-E. Transmission of a heterologous clade C *Symbiodinium* in a model anemone infection system via asexual reproduction. *PeerJ* **2016**, *4*, 2358. [[CrossRef](#)]
10. Rodriguez-Lanetty, M.; Scaramuzzi, C.; Quinnell, R.G.; Larkum, A.W.D. Transport of symbiotic zooxanthellae in mesogleal canals of *Zoanthus robustus*? *Coral Reefs* **2005**, *24*, 195–196. [[CrossRef](#)]
11. Rodriguez-Lanetty, M.; Wood-Charlson, E.M.; Hollingsworth, L.L.; Krupp, D.A.; Weis, V.M. Temporal and spatial infection dynamics indicate recognition events in the early hours of a *dinoflagellate*/coral symbiosis. *Mar. Boil.* **2006**, *149*, 713–719. [[CrossRef](#)]
12. Raz-Bahat, M.; Erez, J.; Rinkevich, B. In Vivo light-microscopic documentation for primary calcification processes in the *hermatypic* coral *Stylophora pistillata*. *Cell Tissue Res.* **2006**, *325*, 361–368. [[CrossRef](#)]
13. Coffroth, M.A.; Poland, D.M.; Petrou, E.L.; Brazeau, D.A.; Holmberg, J.C. Environmental Symbiont Acquisition May Not Be the Solution to Warming Seas for Reef-Building Corals. *PLoS ONE* **2010**, *5*, e13258. [[CrossRef](#)]
14. Brown, B.E. Coral bleaching: Causes and consequences. *Coral Reefs* **1997**, *16*, S129–S138. [[CrossRef](#)]
15. Gateño, D.; Israel, A.; Barki, Y.; Rinkevich, B. *Gastrovascular* Circulation in an Octocoral: Evidence of Significant Transport of Coral and Symbiont Cells. *Boil. Bull.* **1998**, *194*, 178–186. [[CrossRef](#)]
16. Parrin, A.P.; Goulet, T.L.; Yaeger, M.A.; Bross, L.S.; McFadden, C.S.; Blackstone, N.W. Symbiodinium migration mitigates bleaching in three octocoral species. *J. Exp. Mar. Boil. Ecol.* **2016**, *474*, 73–80. [[CrossRef](#)]
17. Marfenin, N.N. Non-radial symmetry of the transport system of *Acropora* corals. *Invertzool* **2015**, *12*, 53–59. [[CrossRef](#)]
18. Gladfelter, E.H. Circulation of fluids in the *gastrovascular* system of the reef coral *acropora cervicornis*. *Boil. Bull.* **1983**, *165*, 619–636. [[CrossRef](#)]
19. Santos, S.R.; Toyoshima, J.; Iii, R.A.K. Spatial and temporal dynamics of symbiotic *dinoflagellates* (*Symbiodinium: Dinophyta*) in the perforate coral *Montipora capitata*. *Galax-J. Coral Reef Stud.* **2009**, *11*, 139–147. [[CrossRef](#)]
20. Camaya, A.P.; Sekida, S.; Okuda, K. Changes in the *Ultrastructures* of the Coral *Pocillopora damicornis* after Exposure to High Temperature, Ultraviolet and Far-Red Radiation. *Cytologia* **2016**, *81*, 465–470. [[CrossRef](#)]
21. Pearse, V.B.; Muscatine, L. Role of symbiotic algae (*zooxanthellae*) in coral calcification. *Boil. Bull.* **1971**, *141*, 350–363. [[CrossRef](#)]
22. Rinkevich, B.; Loya, Y. Does light enhance calcification in *hermatypic* corals? *Mar. Boil.* **1984**, *80*, 1–6. [[CrossRef](#)]
23. Fang, L.-S.; Chen, Y.-W.J.; Chen, C.-S. Why does the white tip of stony coral grow so fast without zooxanthellae? *Mar. Boil.* **1989**, *103*, 359–363. [[CrossRef](#)]
24. Shafir, S.; Van Rijn, J.; Rinkevich, B. Nubbing of Coral Colonies: A Novel Approach for the Development of Inland Broodstocks. *Aquar. Sci. Conserv.* **2001**, *3*, 183–190. [[CrossRef](#)]

25. Shafir, S.; Van Rijn, J.; Rinkevich, B. The use of coral nubbins in coral reef ecotoxicology testing. *Biomol. Eng.* **2003**, *20*, 401–406. [[CrossRef](#)]
26. Shaish, L.; Abelson, A.; Rinkevich, B. How Plastic Can Phenotypic Plasticity Be? The Branching Coral *Stylophora pistillata* as a Model System. *PLoS ONE* **2007**, *2*, e644. [[CrossRef](#)]
27. Shafir, S.; Rijn, J.V.; Rinkevich, B. Steps in the construction of underwater coral nursery, an essential component in reef restoration acts. *Mar. Biol.* **2006**, *149*, 679–687. [[CrossRef](#)]
28. Shafir, S.; Rijn, J.V.; Rinkevich, B. Coral nubbins as source material for coral biological research: A prospectus. *Aquaculture* **2006**, *259*, 444–448. [[CrossRef](#)]
29. Kohler, K.E.; Gill, S.M. Coral Point Count with Excel extensions (CPCe): A Visual Basic program for the determination of coral and substrate coverage using random point count methodology. *Comput. Geosci.* **2006**, *32*, 1259–1269. [[CrossRef](#)]
30. Baruch, R.; Avishai, N.; Rabinowitz, C. UV incites diverse levels of DNA breaks in different cellular compartments of a branching coral species. *J. Exp. Biol.* **2005**, *208*, 843–848. [[CrossRef](#)]
31. Holmes, G.; Osborn, J.; Veal, C.J.; Hoegh-Guldberg, O.; Nunez, M. A comparative study of methods for surface area and three-dimensional shape measurement of coral skeletons. *Limnol. Oceanogr. Methods* **2010**, *8*, 241–253.
32. Fitt, W.K.; Spero, H.J.; Halas, J.; White, M.W.; Porter, J.W. Recovery of the coral *Montastrea annularis* in the Florida Keys after the 1987 Caribbean “bleaching event”. *Coral Reefs* **1993**, *12*, 57–64. [[CrossRef](#)]
33. Littman, R.A.; Van Oppen, M.J.; Willis, B.L. Methods for sampling free-living *Symbiodinium* (zooxanthellae) and their distribution and abundance at Lizard Island (Great Barrier Reef). *J. Exp. Mar. Biol. Ecol.* **2008**, *364*, 48–53. [[CrossRef](#)]
34. Tang, E.P.Y. Why do *dinoflagellates* have lower growth rates? *J. Phycol.* **1996**, *32*, 80–84. [[CrossRef](#)]
35. Wilkerson, F.P.; Parker, G.M.-; Muscatine, L. Temporal patterns of cell division in natural populations of endosymbiotic algae. *Limnol. Oceanogr.* **1983**, *28*, 1009–1014. [[CrossRef](#)]
36. Camaya, A.P. Growth, Cell Division and Dysfunction of Coral Tissues and Symbiotic *Zooxanthellae* in the Scleractinian *Pocillopora damicornis* (Linnaeus) Revealed by Light and Electron Microscopy. Ph.D. Thesis, Kochi University, Kochi, Japan, 2017.
37. Hirose, M.; Yamamoto, H.; Nonaka, M. Metamorphosis and acquisition of symbiotic algae in *planula* larvae and primary polyps of *Acropora* spp. *Coral Reefs* **2008**, *27*, 247–254. [[CrossRef](#)]
38. Kass-Simon, G.S.A.A.; Scappaticci, A.A., Jr. The behavioral and developmental physiology of nematocysts. *Can. J. Zool.* **2002**, *80*, 1772–1794. [[CrossRef](#)]
39. Hennige, S.J.; Smith, D.J.; Perkins, R.; Consalvey, M.; Paterson, D.M.; Suggett, D.J. Photoacclimation, growth and distribution of massive coral species in clear and turbid waters. *Mar. Ecol. Prog. Ser.* **2008**, *369*, 77–88. [[CrossRef](#)]



© 2019 by the authors. Licensee MDPI, Basel, Switzerland. This article is an open access article distributed under the terms and conditions of the Creative Commons Attribution (CC BY) license (<http://creativecommons.org/licenses/by/4.0/>).